

Accepted by the faculty of the Department of Physics and Astronomy, James Madison University, in fulfillment of the requirements for the Honors College

FACULTY COMMITTEE:

Dr. Anca Constantin
Professor, Department of Physics and Astronomy

Dr. Harold Butner
Professor, Department of Physics and Astronomy

Dr. Sean Scully
Professor, Department of Physics and Astronomy

Dr. Bethany Blackstone
Dean, Honors College

**Mid-Infrared Variability of
Galaxies Surveyed for H₂O Megamaser Emission**

An Honors College Project

Presented to the faculty of the Undergraduate

College of Science and Mathematics

James Madison University

by

E. J. McPike

May 2nd, 2024

© Copyright by E. J. McPike May 2nd, 2024

All Rights Reserved

CONTENTS

Abstract	xi
1. Introduction	1
1.1 Significance of Water Megamaser Disks	2
1.2 Surveys for Water Megamaser Emission	5
1.3 AGN Review & Selection of AGN in the Mid-Infrared	8
1.4 AGN Selection with Variability	10
2. Galaxy Sample and Data Collection	13
2.1 Maser & Nonmaser Galaxies	13
2.2 Mid-Infrared Observations	13
2.3 General WISE properties of the MCP samples	15
3 Quantifying Mid-Infrared Variability in Galaxies Surveyed for Maser Emission	18
3.1 Quantifying Variability	18
3.2 Mid-IR Variability and the Water Maser Emission	22
4 Conclusions	27
Bibliography	29
A Maser-AGN Connection	35
A.1 Open Questions in the Maser-AGN Connection	35

LIST OF TABLES

2.1	Cross-matching results between the MCP and WISE catalogs	15
2.2	Mean and standard deviations of the WISE colors presented in Figure 2.1, along with the $\langle W3-W4 \rangle$	17
2.3	Numbers of all masers, megamasers, and disks within the various WISE AGN selection criteria; detection rates are indicated in parentheses	17
3.1	Mean and standard deviations of WISE colors for the subsample of variable galaxies.	22
3.2	Fraction of all variable masers, megamasers, and disks within the WISE AGN selection criteria; detection rates are indicated in parentheses	22

LIST OF FIGURES

- 1.1 Upper Panel: Model of a 3D thin, warped Keplerian disk fitted to the spatial distribution of water maser emission detected in NGC 4258. Lower Panel: The spectrum of the luminous H₂O maser, revealing the high-velocity features on either side of the systemic velocity (470 km s⁻¹); the inset displays the rotation curve of the maser emission, i.e., the line-of-sight velocity versus the impact parameter (distance from the center of the disk). The high-velocity masers outline a Keplerian curve to better than 1% (Herrnstein et al. 1999). 4
- 1.2 Whisker plot that displays a range of 68% confidence level constraints of the Hubble constant H_0 , and a review of direct and indirect models by various astronomical collaborations performed from 2016 - 2021. The cyan vertical band corresponds to the H_0 value from Riess et al. 2019 ($H_0 = 73.2 \pm 1.3$ km/s/Mpc) and the light pink vertical band corresponds to the H_0 value as reported by Planck 2018 team (Aghanim N et al. 2020) within a Λ CDM scenario (Valentino et al. 2021). 7
- 1.3 Distribution of different types of galaxies, from star-forming ones usually inhabiting spiral hosts, to various types of AGNs, like QSOs, Seyferts, LINERs, LIRGs and ULIRGs (and T-dwarfs, which are not relevant for this work) as a function of their WISE $W1 - W2$ and $W2 - W3$ colors. 9

2.1	Distribution of maser and non-maser galaxies as a function of their WISE $W1 - W2$ and $W2 - W3$ colors. Mid-IR AGN criteria are indicated by horizontal dot-dashed lines (i.e., $W1 - W2 \geq 0.5$, or more conservatively $W1 - W2 \geq 0.8$; Ashby et al. 2009 , Stern et al. 2011), along with a more stringent color-color wedge (dashed line) from Mateos et al. (2012).	16
3.1	<i>Left panel:</i> Distribution of Pearson’s correlation coefficient r between $W1$ and $W2$ for all masers and nonmasers. <i>Right panel:</i> Distribution of Pearson’s correlation coefficient between $W1$ and $W2$ for all masers, megamasers, and disks. The delimitation of Pearson $r \geq 0.75$ is shown by a red line in both panels.	19
3.2	Light curves in $W1$, $W2$ and the $W1 - W2$ color for disk maser galaxy J1346+5228, which has $r_{NEOWISE} = 0.50$ and $r_{MEP+NEOWISE} = 0.80$. Because $W1$ and $W2$ do not vary against each other to the same extent in the NEOWISE duration as it does during total observation time, we exclude this galaxy and others with these conditions from being deemed variable.	20
3.3	Individual values of r calculated over the total observation time (WISE Multi-epoch and NEOWISE) plotted against calculated based off of solely NEOWISE data. We chose galaxies that have both $r_{NEOWISE} \geq 0.75$ (horizontal red line) and $r_{NEOWISE+MEP} \geq 0.75$ (vertical red line) to be variable	21

3.4 Distribution of variable ($r_{NEOWISE}$ & $r_{MEP+NEOWISE} \geq 0.75$) maser and non-maser galaxies as a function of their WISE $W1 - W2$ and $W2 - W3$ colors. Mid-IR AGN criteria are indicated by horizontal dot-dashed lines (i.e., $W1 - W2 \geq 0.5$, or more conservatively $W1 - W2 \geq 0.8$; Ashby et al. 2009 , Stern et al. 2011), along with a more stringent color-color wedge (dashed line) from Mateos et al. (2012). 23

3.5 Light curve for the 8 disk masers identified as variable; Three of them (MRK 1029, J0350-0127, NGC 2273) have not been identified as AGN based on their single-epoch mid-IR colors. 24

3.6 Fraction of masers and nonmasers that spend more than 10% of the duration of observation with $W1 - W2 \geq 0.5$ (first row), with $W1 - W2 \geq 0.8$ (2nd row), and within the Mateos et al. wedge (3rd row). *Left panels* show the fractions for the whole samples while *Right panels* show the fractions for the variable sources only. 26

ACKNOWLEDGMENTS

This thesis would not have been possible without the help of my thesis advisor, Dr. Anca Constantin. I would also like to thank my readers for this thesis: Dr. Harold Butner and Dr. Sean Scully. I would like to thank University of North Carolina Chapel Hill undergraduate Anish Aradhey as an amazing collaborator on this project.

This research has made use of the Extragalactic 22 GHz Maser Catalog and ASCII catalog of galaxies surveyed with GBT provided by the Megamaser Cosmology Project (MCP), an NRAO Key Science Project and international effort to constrain the Hubble constant in the local universe. This research has made use of NASA's Astrophysics Data System and of the NASA/IPAC Extragalactic Database (NED) which is operated by the Jet Propulsion Laboratory, California Institute of Technology, under contract with the National Aeronautics and Space Administration. The data products employed in this thesis have been obtained from the Wide-field Infrared Survey Explorer (WISE) and the SDSS. WISE is a joint project of the University of California, Los Angeles, and the Jet Propulsion Laboratory/California Institute of Technology, funded by the National Aeronautics and Space Administration. SDSS is managed by the Astrophysical Research Consortium for the Participating Institutions of the SDSS-III Collaboration including the University of Arizona, the Brazilian Participation Group, Brookhaven National Laboratory, Carnegie Mellon University, University of Florida, the French Participation Group, the German Participation Group, Harvard University, the Instituto de Astrofisica de Canarias, the Michigan State/Notre

Dame/JINA Participation Group, Johns Hopkins University, Lawrence Berkeley National Laboratory, Max Planck Institute for Astrophysics, Max Planck Institute for Extraterrestrial Physics, New Mexico State University, New York University, Ohio State University, Pennsylvania State University, University of Portsmouth, Princeton University, the Spanish Participation Group, University of Tokyo, University of Utah, Vanderbilt University, University of Virginia, University of Washington, and Yale University. This research has made use of the NASA/IPAC Extragalactic Database (NED) which is operated by the Jet Propulsion Laboratory, California Institute of Technology, under contract with the National Aeronautics and Space Administration. Funding for SDSS has been provided by the Alfred P. Sloan Foundation, the Participating Institutions, the National Science Foundation, and the U.S. Department of Energy Office of Science.

This work has been supported by JMU's Physics and Astronomy Department and the National Science Foundation award NSF:AST #1814594.

ABSTRACT

Microwave amplification by stimulated emission of radiation, or maser, is the microwave analog of a laser and originate in star formation regions, shocked interstellar gas, and keenly, within regions closely surrounding matter falling onto supermassive black holes in galaxy centers. When originating from galaxy centers, this emission is millions of times more luminous than detected in association with star formation (and it is therefore called a megamaser), and when it is found in a disk-like configuration, it proves immensely valuable for: (1) uniquely probing the inner works of an active galactic nucleus (AGN; supermassive black holes actively accreting matter onto them) and providing accurate measurements of the mass of the supermassive black hole (SMBH), as well as (2) offering a direct estimate of the value of the Hubble constant in the local universe via geometric angular distance measurements. Unfortunately, water megamaser disks have proved to be exceedingly rare, with a current detection rate of far less than 1% (among a similarly low detection rate of 3% for any type of central water maser emission). For more efficient future searches for water masers, we need a closer look at the conditions in which these emissions originate. Currently, there is tentative evidence proposing a link between the maser pumping mechanism and the AGN activity, however given the varied ways in which AGN activity is detected and the way this is wavelength dependent thanks in part to nuclear and host obscuration, there is no clear indication of how one determines the other. Because the UV and optical emission from the matter accreting onto the SMBH goes

on to be absorbed by surrounding toroidal dust and re-emitted in the mid-infrared, flux variations present in this accretion disk give rise to variability in the mid-infrared. Herein, we investigate the degree to which AGN activity, as probed by mid-infrared variability, correlates with water maser emission and its properties. Mid-infrared observations offer the advantage of being less sensitive to cosmic obscuration, revealing AGN signatures that are missed in other wavelengths. We work here with the Megamaser Cosmology Project (MCP), which offers the most up-to-date list of galaxies surveyed for water maser emission, as well as a decade of multi-epoch mid-infrared data from Wide-field Infrared Survey Explorer (WISE) and present a comparative analysis of variability in galaxies with and without maser emission in their centers.

1. INTRODUCTION

Cosmic masers are natural microwave amplifiers by stimulated emission of radiation. Microwave amplification by stimulated emission of radiation, or maser, is the microwave analog of a laser and is found within star formation regions and, keenly, within parsecs of accreting supermassive black holes (SMBH; $M_{BH} \simeq 10^6 - 10^9 M_{\odot}$; Salpeter 1964, Lynden-Bell 1969). Initially found in stellar formation regions within the spiral arms our own Galaxy, water maser emission is characterized by emission frequency $\nu = 22.2$ GHz ($\lambda = 1.35$ cm). Very powerful maser emissions, with luminosities greater than 10^6 times those of typical galactic sources (hence, "megamasers"), have been detected in the circumnuclear regions of a select population of external galaxies (Dos Santos & Lepine 1979; Baan, Wood & Haschick 1982; Claussen, Heiligman & Lo 1984; Claussen & Lo 1986).

Within circumnuclear regions of galaxies hosting central water megamaser emission, warm, gaseous H_2O exists in a relatively dense state ($T \approx 1000K$, $n(H_2) \approx 10^7 cm^{-3}$) and thus can exist easily outside of thermal equilibrium. In order for the emission to occur, an energy source (e.g., infrared radiation or collisions with other particles) excites water molecules from their lower rotational energy levels to higher levels. This excitation increases the number of molecules in the higher energy state, creating a population inversion. Accretion of matter around SMBHs in galaxy centers acts as this energy source, inducing population inversion within accumulated dense molecular water and resulting in the emission of strong microwave radiation. When a water molecule in the higher energy state collides with another water molecule in

the same condition, it can result in the stimulated emission of a microwave photon in phase with the incident photon. This process leads to the amplification of microwave radiation at the specific frequency ($\nu = 22.2$ GHz) corresponding to the 6_{16} and 5_{23} rotational transition of molecular H_2O . When the radiation occurs over suitably large (~ 1 AU) distances, the emission is able to attain significant amplification, therefore achieving large intensity levels needed for detection (Lo, K.Y. 2005).

1.1 SIGNIFICANCE OF WATER MEGAMASER DISKS

Continuous searches for circumnuclear water megamaser emission revealed tentative evidence that the seed photons needed for emission originate within parsecs of active galactic nuclei (AGN), where there is matter actively accreting around SMBHs in an accretion disk. Considering the proposed parsec scale of circumnuclear accretion disks surrounding AGNs (Antonucci & Miller 1985) and analogous to circumstellar disks suggested as the origin of masers around protostars (Elmegreen & Morris 1979), previous studies have put forth the idea that luminous water maser emission detected in galactic centers could originate within dense gas H_2O clouds apart of this circumnuclear disk (Claussen & Lo 1986). In this model, the molecules within these clouds are excited by a significant mass/energy outflow from a central engine, in this case, accreting SMBHs. Luminous H_2O masers are located in molecular accretion disks and the associated outflow within the central parsec, or in the molecular gas excited by radio jets within tens of parsecs of the center. These megamasers constitute direct evidence for high-density molecular gas very close to the AGN. Although these jets are not completely relevant to this study, they serve as key probes of AGN activity.

This model was evidenced by sub-milli-arc-second resolution observations provided by the Very Long Baseline Interferometry (VBLI), as well as the Very Long Baseline Array (VLBA), observations from both providing a powerful tool to probe spatial

and kinematic distributions of molecular gas in distant galactic nuclei at scales below one parsec.

The combination of bright water megamaser emission and the high angular resolution of VBLA has allowed for an unprecedented probe of an AGN system. Mapping of the water megamaser emission in the circumnuclear region of active galaxy NGC 4258 provided the first direct evidence in an AGN for (i) the existence of a thin Keplerian disk with turbulence and (ii) compelling evidence for the existence of a massive black hole (BH). Figure 1.1 describes the observations provided by the VLBA along with modeling of the associated data, which proves at high confidence that the velocity of the emitting gas falls off from the center of rotation as $r^{-1/2}$ (Greenhill et al. 1995, Miyoshi et al. 1995, Moran et al. 1995), allowing a fit of a nearly edge-on thin Keplerian disk.

Modeling the data provided by the VBLA has allowed for probing of BH masses and direct cosmological distance measurements. This warped disk model has provided the most accurate determinations of central SMBHs, making this model an incredibly accurate dynamical tracer of BHs lying in the centers of distant galaxies (e.g., Lo, K.Y. 2005). Not only have these observations unlocked the mass of NGC 4258's SMBH, but the three-spectra disk-like formation of the emission has also provided single-step distance measurements via direct geometric angular diameter distance measurements. When found in a disk-like formation, water megamasers (disk masers from here on) prove to be a valuable tool for highly accurate and precise constraints of the Hubble Constant (H_0) in the nearby universe (at $z \approx 0$). These measurements are independent, and thus do not involve indirect approximations or assumptions about the physical nature of standard candles and distance ladders (e.g. Reid et al. 2012). An independent constraint of H_0 would help studies limit how fast our universe is expanding, as well as further our understanding of how the universe formed and

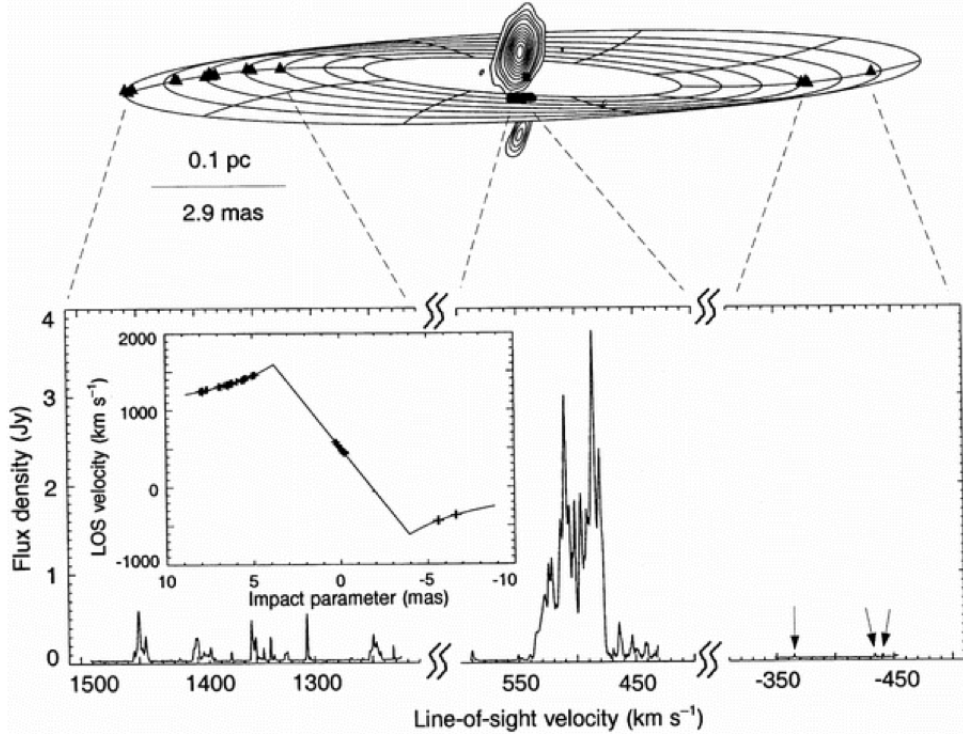


Figure 1.1: Upper Panel: Model of a 3D thin, warped Keplerian disk fitted to the spatial distribution of water maser emission detected in NGC 4258. Lower Panel: The spectrum of the luminous H_2O maser, revealing the high-velocity features on either side of the systemic velocity (470 km s^{-1}); the inset displays the rotation curve of the maser emission, i.e., the line-of-sight velocity versus the impact parameter (distance from the center of the disk). The high-velocity masers outline a Keplerian curve to better than 1% (Herrnstein et al. 1999).

continues to evolve.

Given these findings, it becomes clear that megamaser disks prove immensely valuable as they can (i) uniquely probe the inner works of AGN systems and provide the most accurate masses of the SMBHs that lie within them, and (ii) offer the most promising prospect for obtaining a highly accurate value of H_0 in the local universe via direct geometric angular diameter distance measurements. This allows a direct, single step distance measurement, providing essential alternatives to indirect methods that rely on standard candles and distance ladders.

A $3-\sigma$ or better accuracy in measuring H_0 would provide arguably the best single

constraint on the nature of Dark Energy (DE) where it is most readily detected (Hu 2005; Olling 2007). Unfortunately, disk masers have proved to be extremely rare, with a detection rate of far less than 1% to date (along with a similarly low detection rate of $\gtrsim 3\%$ for any type of central water maser emission). Evidently, searches for additional luminous circumnuclear H₂O masers have proven to be quite challenging. Considering this, we find a stringent need to extend measurements of this phenomenon to more galaxies, motivating this study and the search for clues leading to the potential discovery of additional luminous circumnuclear H₂O megamasers.

1.2 SURVEYS FOR WATER MEGAMASER EMISSION

The Megamaser Cosmology Project (MCP¹) hosts the most extensive catalog of water maser emission at $\nu \approx 22.2$ GHz in galaxy centers. This international collaboration, along with outside additional searches for this phenomenon, only garnered 180 confirmed host galaxies out of ~ 6300 entries in their all-surveyed collection of galaxies. Among the galaxies with detected 22.2 GHz emission, $\sim 80\%$ are luminous enough to be considered megamasers. Furthermore, only $\sim 30\%$ of the megamaser galaxies show the iconic triple spectra, displaying systemic, redshifted, and blueshifted high-velocity emission indicative of a disk-like configuration. The MCP has measured these idyllic galaxies' masses for their SMBHs, which unlocks insight into BH-galaxy co-evolution (e.g. Kormendy & Ho 2013; Greene et al. 2016).

Unfortunately, only a small percent ($\gtrsim 0.03\%$) of surveyed objects are found to be at distances that lie well within the Hubble flow (> 50 Mpc), and thus with recession velocities that remain unaffected by the peculiar velocity within the local group (e.g., Greene et al. 2010, Kuo et al. 2011, Pesce et al. 2020). This work intends to further water megamaser studies in order to investigate ongoing disagreement between models of the expansion of the universe (e.g. A Cold Dark Matter model and

¹<http://wiki.gb.nrao.edu/bin/view/Main/MegamaserCosmologyProject>

the high- z Hubble diagram). Single step distances from geometrical and kinematic measurements of these disk masers can be modeled and used as a standard ruler for distance measurements well into the Hubble flow without dependence on standard ladders or residual radiation from the big bang (cosmic microwave background; CMB).

Currently, there exist prospects for measuring a $1-\sigma$ H_0 value along with distances to high redshift galaxies via megamaser disk observations. With high resolution data of six megamaser disk hosts within 150 Mpc, the MCP recently constrained H_0 to within $\sim 4\sigma$ for a value of $H_0 = 73.9 \pm 3.0$ km/s/Mpc (Pesce et al. 2020). This value is in agreement with late universe measurements of the Hubble constant (Figure 1.2), and with H_0 constrained via Type 1a supernovae ($H_0 = 74.03 \pm 1.42$ km/s/Mpc; Riess et al. 2019) and strong gravitational lensing systems ($H_0 = 73.3 \pm 1.8$; Wong et al. 2020). However, the MCP H_0 is in tension with indirect, early universe H_0 predictions based on CMB data assuming a flat Λ CDM universe (e.g. $H_0 = 67.03 \pm 0.5$ km/s/Mpc; Planck Collaboration 2020). The divide between early and late universe models of H_0 has been coined the "crisis in cosmology", which suggests new physics beyond the standard Λ CDM model (Adballa et al. 2022).

In the early universe, intensive starbursts and AGN formation in galaxies and mergers could have experienced extremely luminous periods as well as extremely large H_2O maser luminosities. This could have encouraged the production of gigamasers ($L_{H_2O} \geq 10^9$). Distance determination of gigamasers at $z \approx 1 - 2$ can provide an independent measure of how fast the universe is expanding. With the increasing sensitivity of new telescopes and receivers, surveys and high-resolution studies of megamasers and gigamasers will be very important tracers and high-resolution probes of active galactic nuclei, dust-embedded starbursts in the earliest galaxies, and galaxy formation processes in the epoch of very active star formation at $z \approx 2$ and beyond (Lo et al. 2005). In order to further test current models of the maser emission physical

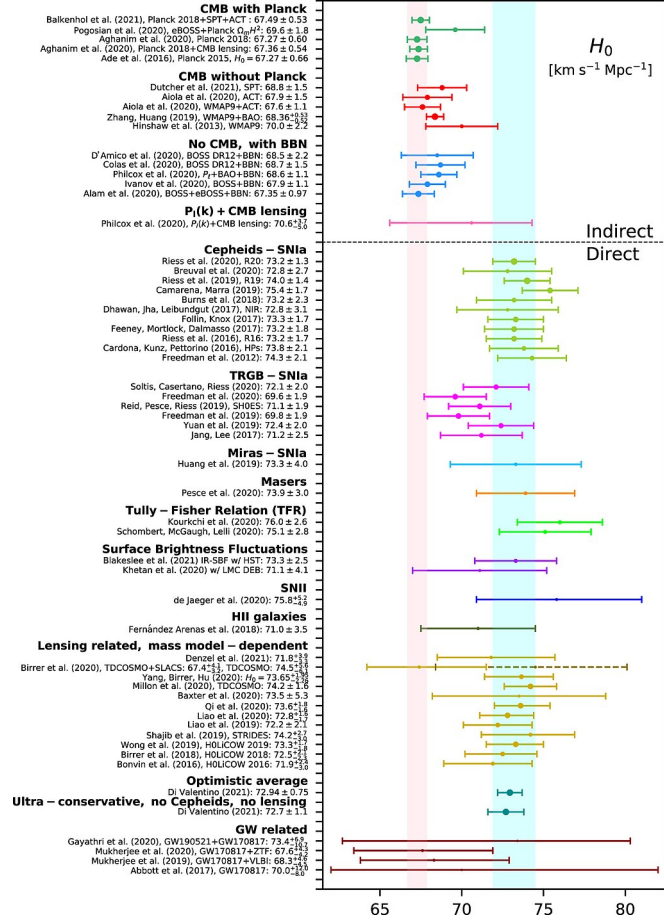


Figure 1.2: Whisker plot that displays a range of 68% confidence level constraints of the Hubble constant H_0 , and a review of direct and indirect models by various astronomical collaborations performed from 2016 - 2021. The cyan vertical band corresponds to the H_0 value from Riess et al. 2019 ($H_0 = 73.2 \pm 1.3$ km/s/Mpc) and the light pink vertical band corresponds to the H_0 value as reported by Planck 2018 team (Aghanim N et al. 2020) within a Λ CDM scenario (Valentino et al. 2021).

properties and pumping mechanism, as well as refine H_0 to increasingly significant accuracy, future surveys for this emission should be able to capture gigamasers from high-z quasars residing in extremely obscured (i.e., Compton-thick) AGNs (Kuo et al. 2020b).

To further employ megamasers as the key dynamical tracers they are, detecting more disk masers is critical. To date, and especially in the most recent years, surveys for these water megamaser disks appear to be unsuccessful in discovering new such

systems, and therefore in significantly increasing their rate of detection. In order to improve the search for this elusive yet crucial phenomenon, we need to better understand the specific physics of these galaxies' central environments, and in particular, find other host galaxy traits that best correlate with the incidence of water megamaser disk emission.

1.3 AGN REVIEW & SELECTION OF AGN IN THE MID-INFRARED

Active galaxies are well known to be dominated by light from their central regions, as light emitted from the accretion of matter onto SMBHs overpowers the total energy output of these galaxies. It follows that the observational signatures of AGN are distinct and cover the entirety of the electromagnetic spectrum. Nevertheless, AGN selection techniques across wavelengths are reliant on various factors, including variations in intrinsic physical properties of AGN, observational/technical facilities, and selection effects like luminosity, morphology, and variability (Lyu et al 2017).

There exists an uncertain fraction of contaminants that may interfere with the true classification of active galaxies (AGN), especially in optical wavelengths. The search for optically concealed AGNs has been significantly alleviated by searches for BH accretion traits in infrared wavelengths (Padavani et al. 2017). Infrared emission has been shown to be particularly useful in identifying these systems, with the best understanding of this type of radiation being the reprocessing of the UV and optical emission from the accretion disk by the circumnuclear toroidal dust which re-emits in the mid-infrared (Lyu et al. 2019).

Surveys like the Wide-field Infrared Survey Explore (WISE) all-sky survey (Wright et al. 2010) allowed for new methods of identifying AGNs that are elusive in other wavebands. WISE mapped the sky in four passbands: $W1$ ($3.4\mu\text{m}$), $W2$ ($4.6\mu\text{m}$), $W3$ ($12\mu\text{m}$), and $W4$ ($22\mu\text{m}$) before running out of solid hydrogen in its outer cryogen tank, after which it continued observations only in the $W1$, $W2$, and $W3$ bands.

WISE studies of galaxy center emission activity have established mid-infrared color criteria that revealed novel populations of AGN, specifically via their red $W1 - W2$ colors (i.e., ≥ 0.5 , or more conservatively ≥ 0.8 ; e.g., Stern et al. 2012), or a three-band AGN wedge in their locus in the color-color diagrams (e.g., Mateos et al. 2014). These approaches significantly broaden the ways in which we can identify bright nuclear accretion activity, enabling the identification of both Type 1 (also known as unobscured, or pole-on viewed AGNs) and Type 2 AGN (missing the broad, thousands of km/s velocity broadening optical emission lines, which is believed to be caused by obscuration of a torus-like geometry of the surrounding dusty torus).

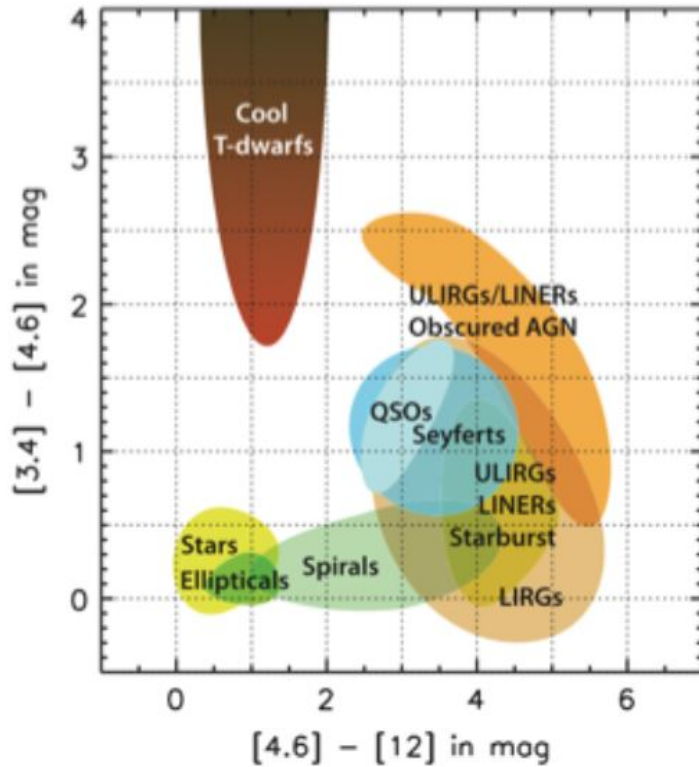


Figure 1.3: Distribution of different types of galaxies, from star-forming ones usually inhabiting spiral hosts, to various types of AGNs, like QSOs, Seyferts, LINERs, LIRGs and ULIRGs (and T-dwarfs, which are not relevant for this work) as a function of their WISE $W1 - W2$ and $W2 - W3$ colors.

WISE-based selection criteria proposed by these studies can even identify heav-

ily obscured AGNs, giving thus a particular advantage over AGN surveys in other wavelengths, which tend to favor unobscured AGNs (e.g., Annunari et al. 2015, 2017; Ricci et al. 2016). Figure 1.3 illustrates how different types of galaxies and other cosmic sources are distributed in terms of two of their WISE mid-IR colors, $W1 - W2$ and $W2 - W3$. Previous studies have shown that while employing mid-IR criteria increases maser detection rates, and while employing mid-IR colors can increase the efficiency in detecting maser emission, these criteria alone are not particularly sensitive or constraining to deciphering the maser pumping mechanism (Witherspoon 2017, Kuo et al. 2018, Kuo et al 2020).

Nevertheless, while single-epoch mid-IR colors provide useful ways of identifying AGN activity, multi-epoch mid-IR observations captured over ~ 10 years may provide a new way of identifying accreting SMBHs even in WISE blue hosts ($W1 - W2 < 0.5$) whose nuclei might host an AGN whose light is overwhelmed or obscured by surrounding blue light, likely coming from surrounding star formation (e.g., Secret & Satyapal 2020). Thus, in this thesis we further the connection between the mid-IR variability as probed by multi-epoch mid-IR observations and the water maser phenomenon, with the main goal of providing a refined way to garner an improved census of potential maser disk targets, via detection of previously hidden AGN in galaxy centers.

1.4 AGN SELECTION WITH VARIABILITY

A popular method for classification of active galaxies is through observing the spectral lines from ionized gas found within tens of parsecs of galaxy centers. Thermally stable nuclear molecular gas is anticipated near AGN (Lepp et al. 1985) and has been inferred through the presence of obscuring dust (high-density gas), as circumnuclear tori (≈ 1 pc scale), from spectro-polarimetric observations (Antonucci & Miller 1985). Luminous water masers are presumed to be located in the molecular

accretion disks and the associated outflow within the central pc, or in the molecular gas excited by radio jets within tens of pc of the center. These mega-masers constitute direct evidence for high-density molecular gas very close to the AGN.

An additional method to identify AGNs is to exploit a well-known facet of AGN: AGN variability at nearly every wavelength. Previous studies have established that AGN are characterized by variability across the electromagnetic spectrum on timescales of hours to years (e.g., Angione 1973; Marshall et al. 1981, Ulrich et al. 1997; Sesar et al. 2007; MacLeod et al. 2010; Kozłowski et al. 2016). Because of this, monitoring variability in prospective AGN can conclusively identify these sources in extragalactic surveys. Time domain AGN observations allow searches for luminosity variability which can detect novel populations of AGN. The cause of the variability is possibly related to instabilities in the accretion disk or surface temperature fluctuations (e.g., Ruan et al. 2014). Interestingly, variability has been found to be stronger in lower luminosity AGNs (Trevese et al. 1994), and this particular property might come handy in our case as the weaker AGNs are associated with the nearby galaxies, where the megamaser emission disk has been detected. Thus, investigating mid-infrared variability in galaxies surveyed for maser emission may aid in elevating the detection rate of the maser emission, as it could illuminate AGN signatures missed by single-epoch WISE-AGN color selections alone. Identifying mid-IR variability in these galaxies could not only further the link between AGN and the incidence of water maser emissions, but could also reveal intrinsic features of maser galaxies that make them more amicable to harboring the emission.

After WISE completely depleted its cryogen supply on September 30, 2010, it briefly continued the mid-IR sky survey in *W1* and *W2* until completely halting operations on February 1, 2011. Nevertheless, following a 3-year hibernation, WISE resumed surveying in only *W1* and *W2* on October 13, 2013 for the NEOWISE

reactivation mission (Mainzer et al. 2014), resulting in a decade of mid-infrared observations. All these data offer an unprecedented opportunity to look not only into how the maser and non-maser galaxies emit in mid-IR, but also into how their emission varies in the time domain, the properties of which prove to be a very useful way of quantifying the presence of AGN activity.

2. GALAXY SAMPLE AND DATA COLLECTION

2.1 MASER & NONMASER GALAXIES

The galaxy sample we use in this thesis are provided by the MCP all-surveyed catalog. Most recently updated in 2018, the catalog data is presented in an atlas containing the positions in the sky, recession velocities, and corresponding references of 180 maser host galaxies. The MCP’s collection encompasses a record of ~ 6300 galaxies that were surveyed for water maser emission, and catalogs include recession velocities, observation sensitivity, and corresponding source brightness temperature. This offers a sample of maser and non-maser galaxies, allowing for a significant statistical comparison of their characteristics. This dataset comprises the largest and most comprehensive catalog of galaxies surveyed for water maser emission at 22 GHz, which can be sub-divided into sub-samples of kilomasers, megamasers, and disk masers, based on their calculated isotropic luminosities and their emission morphologies; see also Table 2.1.

2.2 MID-INFRARED OBSERVATIONS

NASA’s Wide-field Infrared Survey Explorer (WISE; Wright et al. 2010) conducted an all-sky survey, mapping the sky at 3.4, 4.6, 12, and 22 μm ($W1$, $W2$, $W3$, $W4$) in 2010 with an angular resolution of 6.1”, 6.4”, 6.5”, & 12.0” respectively. On the ecliptic in the four bands, WISE has been able to achieve 5 – σ point source sensitivities better than 0.08, 0.11, 1, and 6 mJy in the unconfused regions. Because

of the redundant coverage and less intense zodiacal background, there is a notable sensitivity improvement toward the ecliptic poles. The WISE source catalog includes J2000 positions, photometry, uncertainties, measurement quality flags and extended source and variability flags in the four WISE bands, along with associated information cross-referencing WISE sources with the 2MASS Point and Extended Source Catalogs. We also make use of almost a decade of mid-infrared photometry captured in the NEOWISE Reactivation catalog for our study.

To build our sample, we cross-matched the MCP ASCII catalog of galaxies surveyed with GBT, which contains > 4000 unique galaxies that have been surveyed for water maser emission at 22 GHz, to the AllWISE catalog to within $6''$ for completeness. We then use the AllWISE Multiepoch Photometry (AllWISE MEP) Table and the NEOWISE-R Single Exposure (L1b) Source Table data by matching the AllWISE counterparts coordinates to within $3''$. Notably, the AllWISE MEP sources the offset from the AllWISE catalog are exactly zero for true counterparts. We required a measured SNR > 5 in at least one band for membership in the WISE counterparts of the MCP sources.

We performed a quality control cut: galaxies in MCP ASCII catalog of galaxies surveyed with GBT appear to have been surveyed multiple times. Because of this, we employ name queries to ensure the nonmaser sample is not over-represented. We ensured name queries retained only one source per galaxy by sorting through organizational tags, multiple names, and special characters to eliminate most duplicated galaxies. For galaxies with multiple entries in this catalog, we retained those which were closest to its AllWISE mid-infrared counterparts. These cuts resulted in 4003 nonmaser galaxies from the MCP all surveyed list, with 3626 unique matches in the mid-infrared WISE observations. Cross-matching of maser hosts left 178 unique mid-infrared WISE observations. Finally, within the maser sample, we arranged sub-

samples of 114 megamasers ($L_{H_2O} \geq 10$), and 34 disks. The final numbers of our sample are displayed in Table 2.1.

	Masers	Megamasers	Disks	Nonmasers
MCP	180	116	34	4002
MCP-WISE	178	114	34	3626

Table 2.1: Cross-matching results between the MCP and WISE catalogs

Almost all of the maser galaxies have WISE counterparts, with 100% match in mid-IR for the megamaser disks, illustrating the beautiful coverage available in mid-IR from this survey.

2.3 GENERAL WISE PROPERTIES OF THE MCP SAMPLES

As discussed in Section 1.3, previous studies have put forth limits for WISE $W1-W2$ vs. $W2-W3$ color diagrams which detect significant portions of red/dusty AGNs that do not show AGN-like optical signatures. Because of the novel populations of AGN detected in these surveys, we employ these criteria here to further the connection between obscured AGN activity and water masing activity. Mid-infrared color cuts, which were proposed for identifying red AGNs include $W1 - W2 \geq 0.5$ and $W1 - W2 \geq 0.8$, for a lower contamination by non-active galaxies (Stern et al. 2012) as well as a set of $W1 - W2$ and $W2 - W3$ cuts for the most conservative control for non-AGN contamination by Mateos et al. (2014).

In the case of strong association between megamaser disk emission and obscured AGN activity, one would expect that maser galaxies would populate the $W1-W2 \geq 0.8$ locus from Stern et al. (2012), or three band wedge from Mateos et al. (2012). Additionally, we expect the bulk of the nonmaser sample to fall below the most lenient mid-infrared AGN criteria, $W1-W2 \geq 0.5$ (Stern et al. 2012). This is not immediately apparent in the single-epoch colors (Fig 2.1), as there seems to be con-

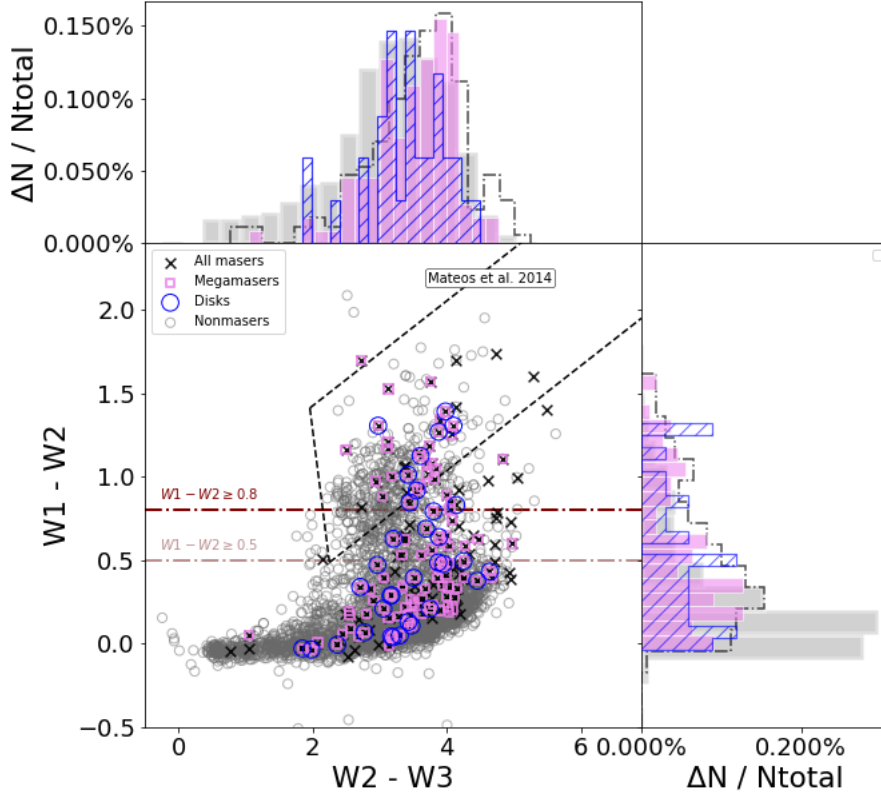


Figure 2.1: Distribution of maser and non-maser galaxies as a function of their WISE $W1 - W2$ and $W2 - W3$ colors. Mid-IR AGN criteria are indicated by horizontal dot-dashed lines (i.e., $W1 - W2 \geq 0.5$, or more conservatively $W1 - W2 \geq 0.8$; Ashby et al. 2009 , Stern et al. 2011), along with a more stringent color-color wedge (dashed line) from Mateos et al. (2012).

siderable overlap between the maser and nonmaser galaxies. Only 26% of all maser galaxies fall within the $W1 - W2 \geq 0.8$ threshold and 20% fall within the Mateos et al. 2012 wedge. While nonmasers populate these areas at a lower rate, $\sim 10\%$ fall within $W1 - W2 \geq 0.8$ or the three band wedge, this is not particularly efficient in constraining the AGN behavior of these systems. Table 2.3 presents the numbers of all masers, megamasers, and disks within the various WISE AGN selection criteria, with the associated detection rates. We list in Table 2.2 the mean values of these colors for the maser and non-maser galaxies, as well as for the subsamples of megamasers and disks; here we see that, in average, maser galaxies are redder in their

$W1 - W2$ colors.

MCP-WISE	$\langle W1-W2 \rangle$	$\langle W2-W3 \rangle$	$\langle W3-W4 \rangle$
All Masers	0.53 ± 0.44	3.57 ± 0.80	2.66 ± 0.44
Megamasers	0.54 ± 0.42	3.51 ± 0.63	2.60 ± 0.40
Disks	0.52 ± 0.42	3.43 ± 0.62	2.59 ± 0.38
Nonmasers	0.26 ± 0.33	3.08 ± 0.93	2.29 ± 0.48

Table 2.2: Mean and standard deviations of the WISE colors presented in Figure 2.1, along with the $\langle W3-W4 \rangle$.

Criteria	All Masers	Megamasers	Disks	Nonmasers
$W1 - W2 \geq 0.5$	73 (42.9%)	47 (42.7%)	13 (38.2%)	672 (18.5%)
$W1 - W2 \geq 0.8$	45 (26.5%)	31 (28.2%)	9 (26.5%)	356 (9.8%)
Mateos et al. (2014)	34 (20.0%)	25 (22.7%)	7 (20.6%)	354 (9.8%)
$W1 - W2 < 0.5$	97 (57.1%)	63 (57.3%)	21 (62.8%)	2954 (81.5%)

Table 2.3: Numbers of all masers, megamasers, and disks within the various WISE AGN selection criteria; detection rates are indicated in parentheses

Looking into AGN variability within the mid-infrared should, however, offer new insights into the AGN – masing activity relation, as mid-IR AGN emission (1–5 μm) contains the signals from the dust reverberation response to the accretion disk variability (Lyu & Rieke 2022). Moreover, infrared wavelengths are relatively less impeded by cosmic obscuration. Therefore, infrared variability is expected to help identify obscured AGNs (Lyu & Rieke 2022). A spearhead investigation into AGN activity as seen by mid-infrared variability was discussed in Secret & Satyapal 2020, which found that mid-infrared variability was not necessarily a good indicator of AGN activity in dwarf galaxies, alluding to differences in their AGN-type of emission from that hosted by more massive galaxies. With mid-infrared variability considered, we expect to see a higher population of maser galaxies within WISE AGN cuts, thereby increasing the detection rate of AGN within maser galaxies.

3 QUANTIFYING MID-INFRARED VARIABILITY IN GALAXIES SURVEYED FOR MASER EMISSION

For the mid-IR $W1$ and $W2$ passbands, we have a suitable coverage of each galaxy to sample light curves for ~ 10 years. In this section, we detail our methods of visualizing the changes in light and quantifying how the $W1$ and $W2$ magnitudes vary against each other over the course of a decade.

3.1 QUANTIFYING VARIABILITY

In order to analyze the variability and properties of mid-infrared light of galaxies with and without maser emission by use of the WISE survey data, we employ non-parametric statistics to determine variability. Following the methodology outlined in Secrest & Satyapal (2020) and Kozłowski et al. (2016, equations 1–3), we calculate the variances, covariances, and Pearson r coefficient between the binned $W1$ and $W2$ measurements in each galaxy’s light curve as a variability metric:

$$r = \frac{C_{m_1, m_2}}{v_{m_1} v_{m_2}},$$

where C_{m_1, m_2} is the covariance between $W1$ and $W2$ for N measurements of a single source:

$$C_{m_1, m_2} = \frac{1}{N-1} \sum_i^N (m_{1,i} - \langle m_1 \rangle) \cdot (m_{2,i} - \langle m_2 \rangle),$$

and v_{m_1} and v_{m_2} are the standard deviations as a function of apparent magnitude in each band for that source:

$$v_m^2 = \frac{1}{N-1} \sum_i^N (m_i - \langle m \rangle)^2,$$

where m_i is the mean magnitude of the source during epoch i , and $\langle m \rangle$ is the mean magnitude of the source in the given band.

This coefficient quantifies the coupling between variation in the $W1$ and $W2$ bands. The distribution of Pearson r coefficients (Figure 3.1) reveals a possible kink starting at $r = 0.75$, so we defined as true variables the objects with $r > 0.75$.

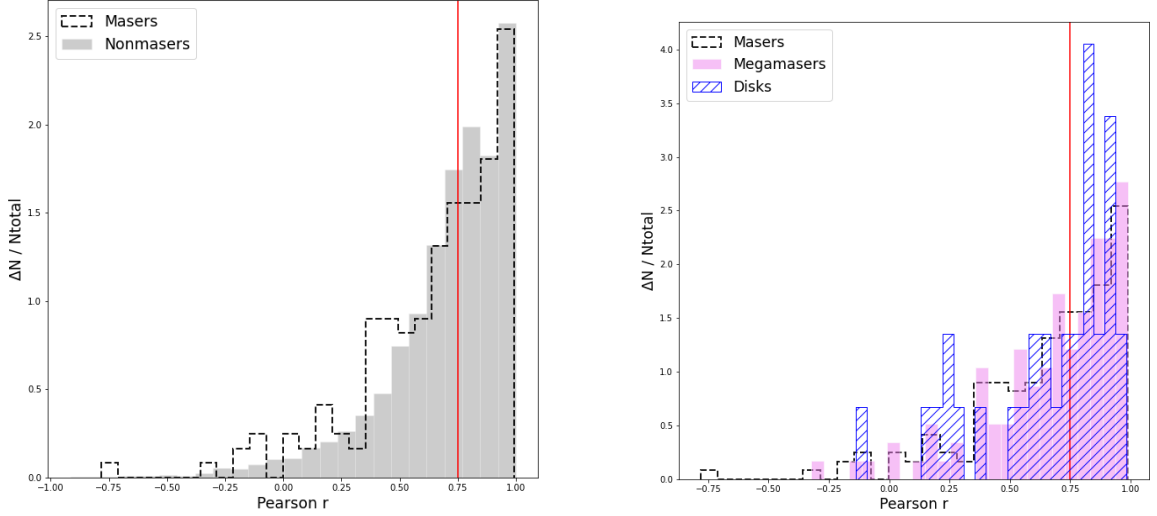


Figure 3.1: *Left panel:* Distribution of Pearson’s correlation coefficient r between $W1$ and $W2$ for all masers and nonmasers. *Right panel:* Distribution of Pearson’s correlation coefficient between $W1$ and $W2$ for all masers, megamasers, and disks. The delimitation of Pearson $r \geq 0.75$ is shown by a red line in both panels.

In certain galaxies like J1346+5228 shown in Fig 3.2, we noted extreme average differences in observations between the Multi-Epoch (MEP) WISE data and the NEOWISE reactivation period variability in a manner that suggests Pearson $r_{MEP+NEOWISE}$ value is mainly dictated by the jump during the WISE hibernation period, but not by intra-year behavior that can be captured during the NEOWISE timeline. Thus, in order to robustly quantify the variability level, we calculated separately the Pearson r coefficients using only NEOWISE data as well as the whole set of observations that cover the total observation time (MEP and NEOWISE), and only deemed a galaxy to be variable if both $r_{NEOWISE}$ and $r_{MEP+NEOWISE}$ had a value ≥ 0.75 .

We show in Fig 3.3 a comparison between the individual r values calculated for

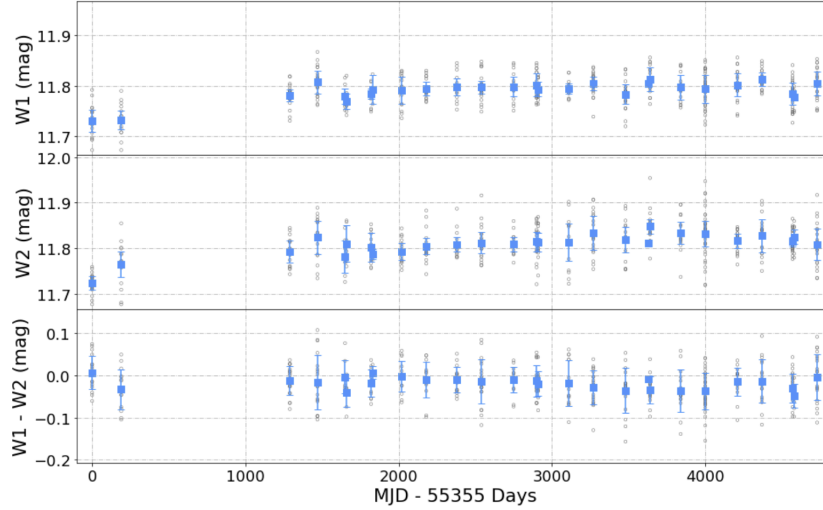


Figure 3.2: Light curves in $W1$, $W2$ and the $W1 - W2$ color for disk maser galaxy J1346+5228, which has $r_{NEOWISE} = 0.50$ and $r_{MEP+NEOWISE} = 0.80$. Because $W1$ and $W2$ do not vary against each other to the same extent in the NEOWISE duration as it does during total observation time, we exclude this galaxy and others with these conditions from being deemed variable.

the two different timelines, where the different types of masers are highlighted with different symbols and colors. Overall, there is a good, one-on-one correspondence between the two coefficients, however, the scatter around it is significant, especially for $r \leq 0.75$. Above this value, however, the two coefficients appear more consistent, which supports our decision to work with $r \geq 0.75$ as a strong measure of variability between $W1$ and $W2$.

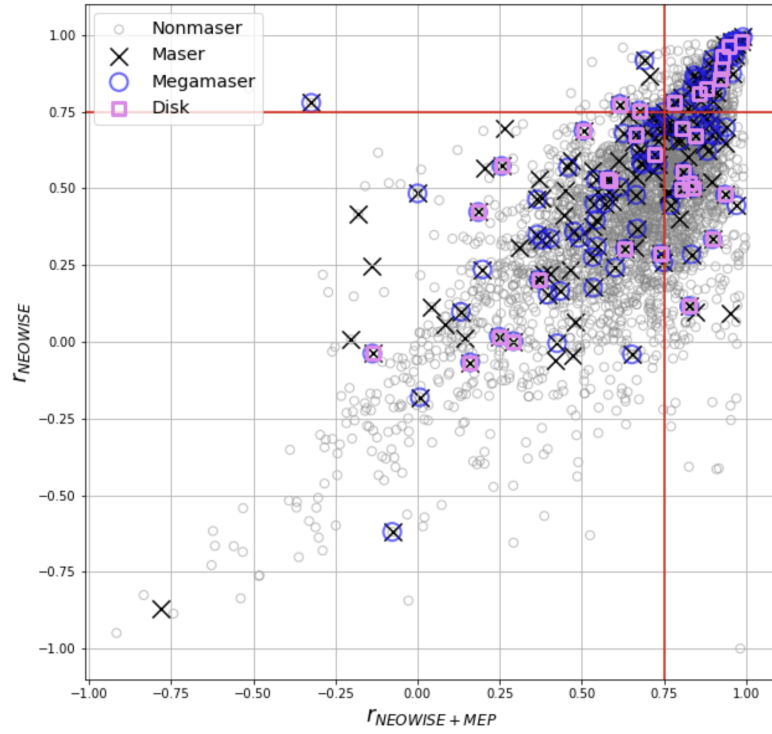


Figure 3.3: Individual values of r calculated over the total observation time (WISE Multi-epoch and NEOWISE) plotted against calculated based off of solely NEOWISE data. We chose galaxies that have both $r_{NEOWISE} \geq 0.75$ (horizontal red line) and $r_{NEOWISE+MEP} \geq 0.75$ (vertical red line) to be variable

3.2 MID-IR VARIABILITY AND THE WATER MASER EMISSION

WISE mid-infrared cuts on the color-color diagram do prove to be a useful tool for identifying red, obscured AGN in maser galaxies, but WISE colors alone do not significantly alleviate the poor detection rate of the blue megamaser disks. However, when considering variability in the mid-infrared, this difficulty is somewhat alleviated. Figure 3.4 illustrates the color-color mid-IR diagram only for the variable MCP galaxies, where it is pretty apparent that a large fraction of blue ($W1 - W2 < 0.5$, or even $W1 - W2 < 0.8$) disks display variability, and therefore are very likely to be associated with an accreting SMBH.

Table 3.1 displays average mid-IR colors for the subsample of variable galaxies. Of the galaxies in our sample, all variable maser galaxies appear to be, on average, much redder in their WISE $W1 - W2$ colors than their nonmaser counterparts.

MCP-WISE	$\langle W1-W2 \rangle$	$\langle W2-W3 \rangle$
All Masers	0.87 ± 0.44	3.54 ± 0.80
Megamasers	0.91 ± 0.42	3.55 ± 0.63
Disks	0.89 ± 0.42	3.68 ± 0.62
Nonmasers	0.5 ± 0.33	3.04 ± 0.93

Table 3.1: Mean and standard deviations of WISE colors for the subsample of variable galaxies.

	Masers	Megamasers	Disks	Nonmasers
$W1 - W2 \geq 0.5$	35 (81.4%)	24 (77.4%)	7 (87.5%)	538 (49.9%)
$W1 - W2 \geq 0.8$	27 (62.8%)	20 (64.5%)	5 (62.5%)	291 (27.0%)
Mateos et al. 2012	23 (53.5%)	18 (58.1%)	4 (50%)	321 (29.8%)
$W1 - W2 < 0.5$	8 (18.6%)	7 (22.6%)	1 (12.5%)	540 (50.1%)

Table 3.2: Fraction of all variable masers, megamasers, and disks within the WISE AGN selection criteria; detection rates are indicated in parentheses

Of the 34 disk galaxies in our sample, we find that 8 are variable in the mid-infrared. We present in Figure 3.5 the 8 disk galaxies that appear to be variable in the mid-IR, pointing out that three of them have $W1 - W2 < 0.8$, and therefore

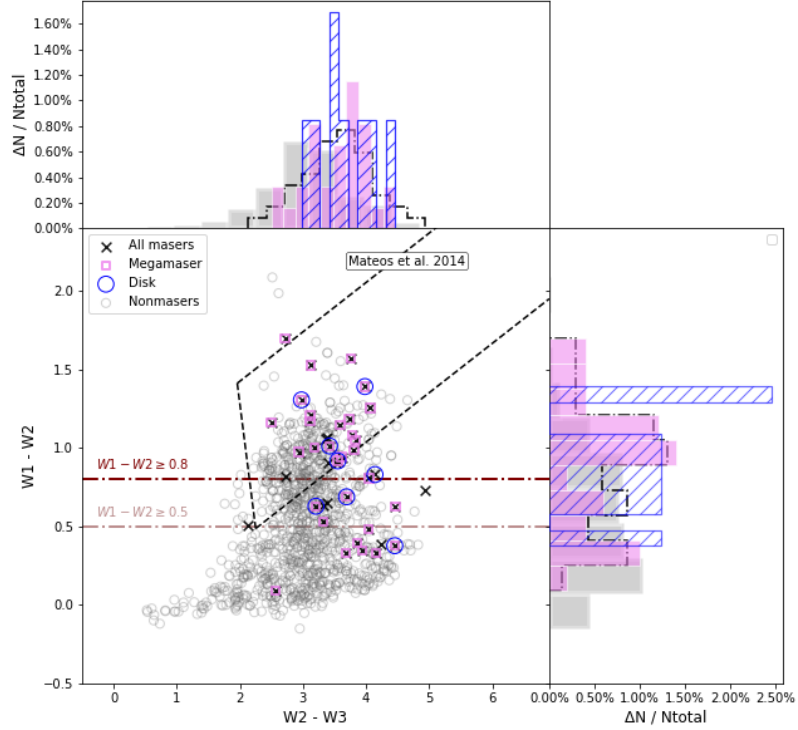
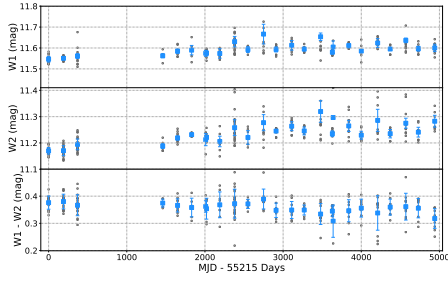
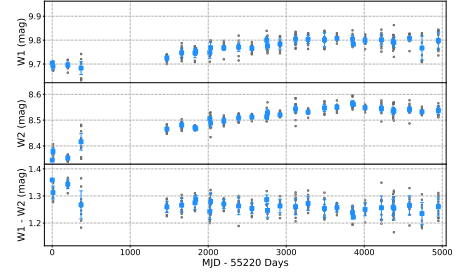


Figure 3.4: Distribution of variable ($r_{NEOWISE} \& r_{MEP+NEOWISE} \geq 0.75$) maser and non-maser galaxies as a function of their WISE $W1 - W2$ and $W2 - W3$ colors. Mid-IR AGN criteria are indicated by horizontal dot-dashed lines (i.e., $W1 - W2 \geq 0.5$, or more conservatively $W1 - W2 \geq 0.8$; Ashby et al. 2009 , Stern et al. 2011), along with a more stringent color-color wedge (dashed line) from Mateos et al. (2012).

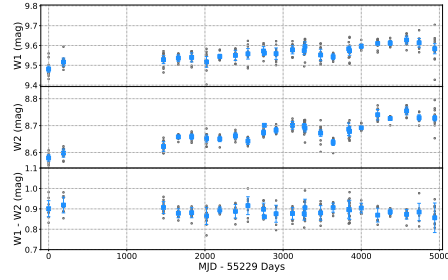
would not have been identified as AGN based on their WISE colors alone. These new variability measures reveals their true AGN nature.



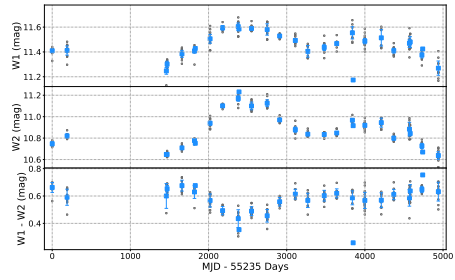
(a) MRK 1029, $r_{NEOWISE} = 0.82$,
 $r_{MEP+NEOWISE} = 0.88$



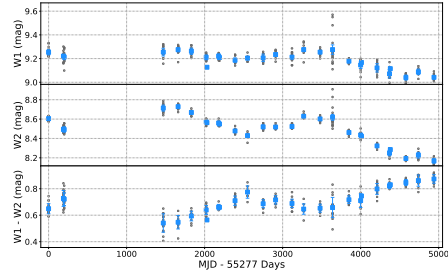
(b) NGC 1194, $r_{NEOWISE} = 0.86$,
 $r_{MEP+NEOWISE} = 0.92$



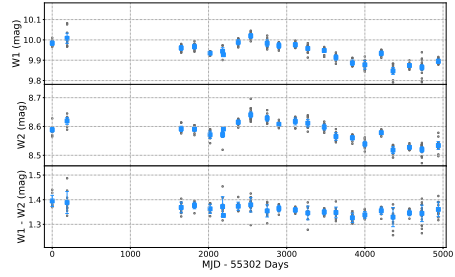
(c) NGC 1320, $r_{NEOWISE} = 0.89$,
 $r_{MEP+NEOWISE} = 0.92$



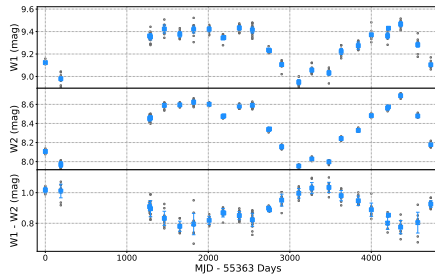
(d) J0350-0127, $r_{NEOWISE} = 0.78$,
 $r_{MEP+NEOWISE} = 0.78$



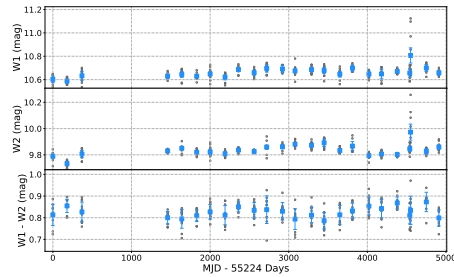
(e) NGC 2273, $r_{NEOWISE} = 0.93$,
 $r_{MEP+NEOWISE} = 0.93$



(f) MRK 1210, $r_{NEOWISE} = 0.96$,
 $r_{MEP+NEOWISE} = 0.95$



(g) NGC 4388, $r_{NEOWISE} = 0.98$,



(h) NGC 5765, $r_{NEOWISE} = 0.81$,
 $r_{MEP+NEOWISE} = 0.86$

Figure 3.5: Light curve for the 8 disk masers identified as variable; Three of them (MRK 1029, J0350-0127, NGC 2273) have not been identified as AGN based on their single-epoch mid-IR colors.

Considering the variability displayed in the mid-infrared by galaxies in our sample, we monitored the duration of time each galaxy spent within WISE AGN criteria. Figure 3.6 displays the fractions of galaxies in each sample which spend a significant portion of their observed time (10%) within the tree specific mid-IR color-color AGN criteria mentioned above. Comparing the distribution of galaxies regardless of variability with those we classified as variable, we see that considering variability greatly increases the fraction of detection of any type of maser galaxy that are classified as AGN by WISE AGN criteria. Although a similar increase is displayed in the nonmaser sample, this pattern is much weaker than that shown by the maser subsamples. This finding supports an intrinsic connection between the maser emission and the AGN nature of their host galaxies.

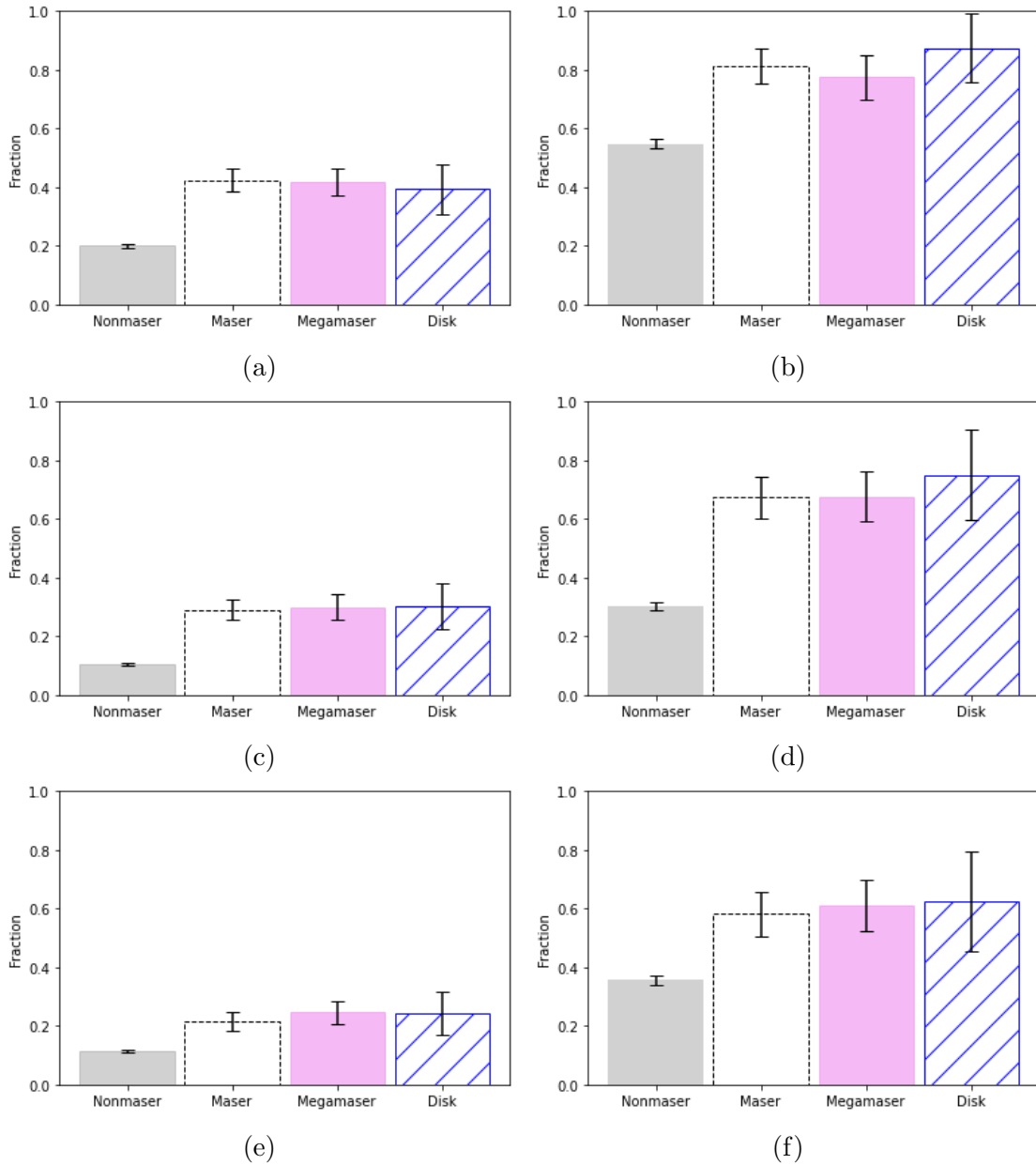


Figure 3.6: Fraction of masers and nonmasers that spend more than 10% of the duration of observation with $W1 - W2 \geq 0.5$ (first row), with $W1 - W2 \geq 0.8$ (2nd row), and within the Mateos et al. wedge (3rd row). *Left panels* show the fractions for the whole samples while *Right panels* show the fractions for the variable sources only.

4 CONCLUSIONS

With the aim of better connecting the incidence of water maser emission with circumnuclear dust absorption and radiative reprocessing in the centers of active galaxies, we have compared the mid-infrared photometric variability of galaxies surveyed for circumnuclear water megamaser emission at 22 GHz. Recalling the low detection rate for water megamaser disks among galaxies surveyed for water megamaser emission, the similarly dismal rate for any type of central water maser emission, and the importance of studying them in detail to improve models of AGN systems and constrain cosmological distances, refining systemic surveys is paramount to increase the amount of masers available to us.

With the mid-IR observations available from WISE, we present a variability analysis of the mid-IR emission of the most comprehensive list of galaxies surveyed for water megamaser emission at 22 GHz in galaxy centers. From our analysis, we determine:

- Of the 34 disk galaxies identified by the MCP, 8 (24%) are considered variable based on their mid-IR emission. When considering the variance between the $W1$ and $W2$ mid-IR WISE passbands, we find that masers display variability at a greater incidence than nonmasers.
- Of the 8 disk masers that display significant mid-infrared variability, 1 is considered star forming when classified by single-epoch mid-infrared colors alone.
- Variable disk masers display distinct AGN behavior, as brightening is associated with a reddening of their WISE $W1 - W2$ colors, which is consistent with increasing AGN dominance over the host galaxy.
- Nonmasers appear bluer than masers regardless of variability.

In conclusion, employing both mid-infrared WISE AGN criteria and mid-infrared variability helps reveal new populations of AGN not previously captured by other surveys, and therefore new connections between AGN and maser activities in galaxy centers. While single-epoch WISE colors may not be particularly effective in constraining the maser pumping mechanism, the relations presented here between megamaser and BH-accretion activities, quantified via variability, may point to thermal heating strengthening the incidence of maser emission in galaxy centers.

BIBLIOGRAPHY

- [1] Huang, W., Ren, Y., & Russell, R. D. (1994). Moving Mesh Methods Based on Moving Mesh Partial Differential Equations. *Journal of Computational Physics*, 113(2), 279-290.
- [2] Dos Santos, P. M., & Lepine, J. R. D. (1979). A southern survey of proper motions in the direction of the Galactic Center. *Nature*, 278(5701), 34.
- [3] Baan, W. A., Wood, P. A., & Haschick, A. D. (1982). Radio observations of the nucleus of NGC 1068. *The Astrophysical Journal Letters*, 260, L52.
- [4] Claussen, M. J., Heiligman, G. M., & Lo, K. Y. (1984). Discovery of a high-velocity molecular jet in W 49. *Nature*, 310(5977), 298.
- [5] Claussen, M. J., & Lo, K. Y. (1986). VLBI observations of water vapor masers in W 49N. *The Astrophysical Journal*, 308, 592.
- [6] Lo, K. Y. (2005). Maser Emission in Star-forming Regions. *Annual Review of Astronomy and Astrophysics*, 43, 625.
- [7] Salpeter, E. E. (1964). Accretion of interstellar matter by massive objects. *The Astrophysical Journal*, 140, 796.
- [8] Lynden-Bell, D. (1969). Galactic Nuclei as Collapsed Old Quasars. *Nature*, 223(5207), 690.

- [9] Antonucci, R. R. J., & Miller, J. S. (1985). Spectropolarimetry and the nature of NGC 1068. *The Astrophysical Journal*, 297, 62.
- [10] Elmegreen, B. G., & Morris, M. (1979). Molecular clouds in the Galactic Center region. *The Astrophysical Journal*, 229, 593.
- [11] Greenhill, L. J., Henkel, C., Becker, R., Wilson, T. L., & Wouterloot, J. G. A. (1995). A disk of molecular gas around a supermassive black hole at the centre of the Galaxy. *Astronomy & Astrophysics*, 304, 21.
- [12] Greenhill, L. J., Jiang, D. R., Moran, J. M., Reid, M. J., Lo, K. Y., & Claussen, M. J. (1995). A molecular disk and jet in 3C 84. *The Astrophysical Journal*, 440, 619.
- [13] Miyoshi, M., Moran, J. M., Herrnstein, J., Greenhill, L., & Nakai, N. (1995). Evidence for a black hole from high rotation velocities in a sub-parsec region of NGC 4258. *Nature*, 373(6510), 127.
- [14] Moran, J. M., Greenhill, L. J., Herrnstein, J., Diamond, P., & Miyoshi, M. (1995). Detection of a molecular disk orbiting the supermassive black hole in M81. *Proceedings of the National Academy of Sciences*, 92(25), 11427.
- [15] Herrnstein, J. R., Moran, J. M., Greenhill, L. J., Diamond, P. J., & Inoue, M. (1999). A geometric distance to the galaxy NGC 4258 from orbital motions in a nuclear gas disk. *Nature*, 400, 539-541.
- [16] Reid, M. J. (2012). Parallax of Galactic masers: Geometric distance determination to star-forming regions. *IAU Symposium*, 287, 359.
- [17] Hu, W. (2005). ALMA: The Atacama Large Millimeter Array. *ASP Conference Series*, 339.

- [18] Olling, R. P. (2007). A simple model for the absorption of H I 21 cm emission by interstellar gas in spiral galaxies. *Monthly Notices of the Royal Astronomical Society*, 378(4), 1385.
- [19] Kuo, C. Y., Braatz, J. A., & Condon, J. J. (2011). The Megamaser Cosmology Project. IV. A direct measurement of the Hubble constant from UGC 3789. *The Astrophysical Journal*, 727, 20.
- [20] Wright, E. L., Eisenhardt, P. R. M., Mainzer, A. M., & Ressler, M. E. (2010). The Wide-field Infrared Survey Explorer (WISE): Mission Description and Initial On-orbit Performance. *The Astronomical Journal*, 740(6), 1868.
- [21] Stern, D., Assef, R. J., & Benford, D. J. (2012). The WISE/SDSS Stripe 82 Quasar Survey. *The Astrophysical Journal*, 753, 30.
- [22] Ashby, M. L. N., Stern, D., Brodwin, M., Grith, R., & Eisenhardt, P. (2009). The Spitzer Wide-area InfraRed Extragalactic (SWIRE) Survey: 5.8 and 8.0 μm and 24 μm Data and Catalogs. *The Astrophysical Journal*, 701, 428.
- [23] Satyapal, S., Secrest, N. J., & McAlpine, W. (2014). The Radio Properties of Radio-quiet Quasars. *The Astrophysical Journal*, 784, 113.
- [24] Aghanim, N., et al. (Planck Collaboration). (2020). Planck 2018 results. VI. Cosmological parameters. *Astron. Astrophys.*, 641, A6.
- [25] Riess, A. G., et al. (2018). Type Ia supernova distances at redshift >1.5 from the Hubble Space Telescope Multi-Cycle Treasury Program: The early expansion rate. *Astrophys. J.*, 855, 136.
- [26] Reid, M. J., Pesce, D. W., & Riess, A. G. (2019). A geometric distance measurement to the galaxy NGC 4258 from orbital motions in a nuclear gas disk. *Astrophys. J. Lett.*, 886, L2.

- [27] Pesce, D. W., et al. (2020). The megamaser cosmology project. XII. VLBI imaging of H₂O maser emission in a low-redshift barred spiral galaxy. *Astrophys. J. Lett.*, 891, L1.
- [28] Assef, R. J., Stern, D., Kochanek, C. S., Blain, A. W., Brodwin, M., et al. (2013). A mid-infrared spectroscopic survey of star-forming galaxies in the local universe. *ApJ*, 772, 26.
- [29] Baan, W. A., Wood, P. A., & Haschick, A. D. (1982). Water vapor maser emission from the nuclear region of NGC 1068. *ApJL*, 260, L52.
- [30] Baldwin, J. A., Phillips, M. M., & Terlevich, R. (1981). Classification parameters for the emission-line spectra of extragalactic objects. *PASP*, 93, 5.
- [31] Bottinelli, L., Fraix-Burnet, D., Gouguenheim, L., Kazes, I., Le Squeren, A. M., et al. (1985). The kinematics of the local universe. *A&A*, 151, L7.
- [32] Braatz, J. A., Wilson, A. S., & Henkel, C. (1996). The megamaser cosmology project. I. Very Long Baseline Interferometric detections of 22 GHz H₂O maser emission in seven active galaxies. *ApJ*, 106, 51.
- [33] Braatz, J. A., Wilson, A. S., & Henkel, C. (1997). The megamaser cosmology project. II. An angular diameter distance to NGC 4258 from observations of water masers. *ApJ*, 110, 321.
- [34] Braatz, J. A., Henkel, C., Greenhill, L. J., Moran, J. M., & Wilson, A. S. (2004). The megamaser cosmology project. III. Accurate masses of seven supermassive black holes in active galaxies with circumnuclear megamaser disks. *ApJ*, 617, L29.
- [35] Braatz, J. A., Reid, M. J., Humphreys, E. M. L., et al. (2010). The megamaser

- cosmology project. IV. A direct measurement of the Hubble constant from UGC 3789. *ApJ*, 718, 657.
- [36] Kuo, C. Y., Braatz, J. A., Condon, J. J., et al. (2011). The megamaser cosmology project. V. Accurate masses of seven supermassive black holes in active galaxies with circumnuclear megamaser disks. *ApJ*, 727, 20.
- [37] Kuo, C. Y., Braatz, J. A., Reid, M. J., et al. (2013). The megamaser cosmology project. VI. Observations of NGC 6323. *ApJ*, 767, 155.
- [38] Kuo, C. Y., Braatz, J. A., Lo, K. Y., et al. (2015). The megamaser cosmology project. VII. Investigating disk physics using spectral monitoring observations. *ApJ*, 800, 26.
- [39] Di Valentino, E., Mena, O., Pan, S., Visinelli, L., Yang, W., Melchiorri, A., Mota, D. F., Riess, A. G., & Silk, J. (2021). In the realm of the Hubble tension—a review of solutions. *Classical and Quantum Gravity*, 38(15)
- [40] Padovani, P., Alexander, D. M., Assef, R. J., De Marco, B., Giommi, P., Hickox, R. C., Richards, G. T., Smolčić, V., Hatziminaoglou, E., Mainieri, V., & Salvato, M. (2017). Active galactic nuclei: what’s in a name? *The Astronomy and Astrophysics Review*, 25(1), 2.
- [41] Lyu, J., Rieke, G. H., & Smith, P. S. (2019). Mid-IR variability and dust reverberation mapping of low-*z* quasars. I. Data, methods, and basic results. *The Astrophysical Journal*, 886(1), 33.
- [42] Kuo, C. Y., Constantin, A., Braatz, J. A., Chung, H. H., Witherspoon, C. A., Pesce, D., Impellizzeri, C. M. V., Gao, F., Hao, L., Woo, J.-H., & Zaw, I. (2018). Enhancing the H₂O megamaser detection rate using optical and mid-infrared photometry. *The Astrophysical Journal*, 860(2), 169.

- [43] Pesce, D. W., Braatz, J. A., Reid, M. J., Condon, J. J., Gao, F., Henkel, C., Kuo, C. Y., Lo, K. Y., & Zhao, W. (2020). The Megamaser Cosmology Project. XI. A geometric distance to CGCG 074-064. *The Astrophysical Journal*, 890(2), 118.
- [44] Lyu, J., & Rieke, G. (2022). Infrared spectral energy distribution and variability of active galactic nuclei: Clues to the structure of circumnuclear material. *Universe*, 8(6), 304.
- [45] Kuo, C. Y., Gao, F., Braatz, J. A., Pesce, D. W., Humphreys, E. M. L., Reid, M. J., Impellizzeri, C. M. V., Henkel, C., Wagner, J., & Wu, C. E. (2023). What determines the physical size of a H₂O megamaser disk?
- [46] Secret, N. J., & Satyapal, S. (2020). A low incidence of mid-infrared variability in dwarf galaxies. *The Astrophysical Journal*, 900(1), 56. doi:10.3847/1538-4357/ab9309.
- [47] Kozłowski, S., Kochanek, C. S., Ashby, M. L. N., Assef, R. J., Brodwin, M., Eisenhardt, P. R., Jannuzi, B. T., & Stern, D. (2016).

A MASER-AGN CONNECTION

A.1 OPEN QUESTIONS IN THE MASER-AGN CONNECTION

There exists a tentative connection between megamaser disk activity and the accretion process within AGN which has existed since the discovery of the megamaser disk in NGC 4258 (Herrnstein et al. 1999). Of the conditions required for maser amplification, high column density along the line of sight can explain the association with narrow line Type 2 AGN (e.g., Braatz et al. 1997b; Kondratko et al. 2006). This condition is especially relevant within Compton-thick systems (e.g., Greenhill et al. 2008; Zhang et al. 2010; Castangia et al. 2013) as it also offers an explanation for the association. Another condition for maser emission, radiative heating necessary for population inversion, may be associated with other processes within circumnuclear regions of active galaxies besides accretion of matter onto SMBHs, as shocks and strong star formation are also able to achieve the same amplification (e.g., Lo 2005).

Considering this, there remains the open question as to whether or not maser disk activity and AGN are intrinsically linked. The link between accretion processes and the origin and temporal longevity of the maser disk emission is also left as an open question. To assume all megamaser disks are associated with the accretion of matter onto SMBHs, it is necessary to understand why certain types of AGN are more likely to host the emission, even within those Type 2 AGN.

Among the open questions that remain surrounding maser disk emission, there exists an unclear link between the emission and the obscuring dusty torus. While maser disks could be located within the innermost edge of a molecular accretion disk adjacent to the torus, the column density necessary for significant amplification could very well be provided by the thin, central plane of the torus. Additionally, it could be dynamically independent from the torus, with a considerable misalignment between

their axes.

This is made even more unclear by quasar J0414+0534, a megamaser host which displays distinct broad line emission (Impellizzeri et al. 2008), pointing to the existence of maser disk emission within broad-lined AGN and implying the incidence of emission is not as contingent on the presence of a torus as originally modelled. Alternatively, furthering the connection between the torus and maser emission, or disproving it, could provide refining characteristics to the AGN unification model, furthering our understanding of the innermost facilities of AGN.

Furthermore, it remains challenging to constrain the dominant ionization mechanism of AGN for a considerable fraction of nearby galaxies, which is necessary to accurately identifying AGN. These challenges are perpetrated by various quandaries: optical spectra reveals line flux ratios that offer little clarity to their true classification as they populate the borders of starburst galaxies and AGNs (e.g., Filippenko & Sargent 1985; Constantin et al. 2015), X-ray emission fails to meet the secure AGN limit of 10^{42} erg/s (e.g., Constantin et al. 2010; Netzer 2015), and only a small fraction of the sample has radio morphology consistent with compact emitters (Merloni 2015). It is important to note while maser detection is highest among Seyferts, it has been shown the detection rate may be due to selection bias rather than a genuine connection between the emission and morphology, as galaxies in maser surveys have focused almost entirely on Type 2 Seyfert galaxies and the maser detection rate is non-zero for non-AGN types (Constantin 2012).

Taking this into consideration, we cannot confidently determine that megamaser disk emission is always produced in association with accretion of matter onto SMBHs or if the emission is reliant on the presence of a dusty/molecular torus. To strengthen the connection between the emission and the presence of this torus, answer open questions in the nature of this elusive emission, and possibly refine future surveys for

this emission, we explore connections between conventional AGN classifications and more than a decade of mid-infrared photometry for galaxies surveyed for water maser emission.